New Metal Complexes Derived from Schiff-Base Ligand: Synthesis Structural Characterisation, Thermal Properties and Biological Evaluation

Raghad Usama Abass[1], and Enaam Ismail Yousif[2]*
1,2Department of Chemistry, College of Education for Pure Science (Ibn Al-Haitham), University of Baghdad, Adhamiyah, Baghdad, Iraq.
Email: enaamismail@yahoo.com

Abstract

New Schiff-base ligand and metal complexes with Cr(Ш), Mn (II), Fe (II), Co (II), Ni (II) and Cu (II) ions are reported. Ligand was prepared in two-step reaction. The reaction of 2-hydroxy-5-methylisophthalaldehyde with 3-Amino-1-propanol resulted in the isolation of precursor (3,3'-((1E,1'E)-(propane-1,3-diylbis (azanylylidene)) bis (methanylylidene)) bis (2-hydroxy-5-methylbenzaldehyde)).The reaction of precursor with 4-Aminoantipyrine gave the required ligand; (4,4'-(((1E,1'E)-(((1E,1'E)(propane-1,3-diylbis(azanylylidene))bis (methanyl ylidene))bis(2-hydroxy-5-methyl-3,1-phenylene)) bis(methanylylidene)) bis(azanyl ylid ene)) bis(1,5-dimethyl-2-phenyl-1,2-dihydro-3H-pyrazol-3-one)) H2L. The reaction of this ligand with the appropriate metal ions gave metal complexes of the formulae [M2(L) (H2O)2 Cl2]. Cl2, M= Cr(Ш), [M2(L)Cl2(H2O)2], M=Mn (II), Fe (II), [M2(L)] Cl2.H2O, M=Co (II), Ni (II), [M2(L)Cl2] H2O, M= Cu (II). A range of techniques were used to confirm the entity of ligand and their complexes. The formation of ligand and mode of complexation and geometrical structure of complexes were verified using FTIR, electronic spectra, NMR, ESMS, magnetic susceptibility, micro-elemental analysis, metal content, chloride content and conductance. The analytical and spectroscopic data indicated the formation of four and six-coordinate for complexes. Biological evaluation of ligand and complexes against gram-positive bacteria (G+), Bacillus stubtili, Staphylococcus aureus, and gram-negative bacteria (G−), Escherichia coli and Pseudomonas aeruginosa and compared with antibiotic drug (Cefotaxime) and two types of fungi namely (Candida albicans and Rhizopus sporium) and compared with the activity of fungal agent (Fluconazole). The collected data revealed the antimicrobial activity of the ligand was enhanced upon complex formation.

Keywords: Schiff-base ligand,4-Aminoantipyrine, Metal complexes, Structural study, biological evaluation.

1. Introduction

Schiff bases are formed by the reaction between primary amine with an aldehyde or a ketone under specific conditions and used as amino protective groups in organic synthesis [1]. The transition metal complexes having oxygen and nitrogen donor Schiff bases possess unusual configuration, structural liability and are sensitive to the molecular environment. Schiff bases play a major role in their significant bioactivities and containing azomethine (-N=CH-) as an active pharmacophore [2]. Schiff bases considered as important starting materials to synthesis new drug design and intermediate in organic syntheses, or rubber additives schiff- base of 4-amino antipyrine and their complexes are known for their variety of application [3,4] in the areas of catalysis clinical application and pharmacology [5-7]. Also, the chemistry of antipyrine and their derivatives has been extensively investigated due to their physiological properties [8-10]. The aim of the present study is to synthesize and characterizes Cr(Ш), Mn (II), Fe (II), Co (II), Ni(II) and Cu(II) metal complexes with newly synthesis Schiff base ligand derived from 4-aminoantipyrine.

2. Experimental

3. Methods and Materials

Substances that obtained from Aldrich were used as usual. Solvents were dried using normal protocols prior to their use in the preparation.

Measurement techniques

Melting points were noted without corrections on an Electro-thermal Meltter Toledo MP90 melting point apparatus. Micro-elemental analyses (C.H.N) were carried out on (Eager 300 for EA1112). The FTIR spectra of compounds were recorded using KBr and CsI discs from 4000–200cm-1 on a Shimadzu Fourier Transform Infrared Spectrometer (FTIR-600). The UV-Vis spectra of samples with 10-3 M concentration in DMSO solutions at room temperature were measured from 200-1100 nm using a Shimadzu 1800 spectrophotometer. A positive mode Electrospray (ES) mass spectroscopy was used to measure the mass spectra for ligand. 1H-NMR spectra was recorded in DMSO-d6 solutions on Brucker 400 MHz spectrometer. Tetramethylsilane (TMS) was used as an internal standard for 1H NMR analysis. The percentage of metals and chloride content were acquired using atomic absorption

doi.org/10.31838/hiv22.02.584 Received: 12.04.22, Revised:24.05.22, Accepted: 11.08.22

spectrophotometer (on a Shimadzu (A.A) 680 G) and potentiometer titration method (on a 686-Titrp processor-665 Dosim A-Metrohm/Swiss), respectively. Molar conductance was performed on a PW 9526 apparatus with DMSO solutions. The magnetic susceptibility measurements were made at room temperature with a magnetic susceptibility balance (Sherwood Scientific). The chloride content for complexes was determined using the potentiometric titration method on 686-Titro Processor-665 Dosim A-Metrohm/Swiss. Thermogravimetric analysis (TGA) was carried out on STA PT-1000 Linseis Company/Germany. The biological evaluation of the ligand and its metal complexes against four bacterial species (Escherichia coli, Pseudomonas aeruginosa, Staphylococcus aureus and Bacillus stubtilis) and compared with antibiotic drug (Cefotaxime) and two types of fungi (Candida albicans and Rhizopus sporium) and compared with the activity of fungal agent (Fluconazole) were performed using agar-well diffusion approach. In this method, the wells were dug in the media with the help of antiseptic metallic borer with centres of at least 6mm. Recommended concentration (100µL) of the test sample of 1mg/mL in DMSO was introduced in the respective wells. The dishes were raised immediately at 37°C for 24h. The activity was calculated by measuring the diameter of reticence zones (mm).

Synthesis

Synthesis of precursor

The preparation of precursor (3,3'-((1E,1'E)-(propane-1,3-diylbis (azanylylidene))bis (methanylylidene))bis (2-hydroxy-5-methylbenzaldehyde)).

A precursor was prepared according to the literature [11]. 3-Amino-1-propanol was added to a EtOH solution 30ml (0.5g, 1.5mmol) was added to 2-hydroxy-5-methylisophthalaldehyde (0.5g, 3.1mmol) with few drops' bromic acid. The resulting solution was refluxed for 4hr and heated at 80°C. The light-yellow precipitate was isolated by filtration. More pure product was obtained by means of washed from hot ethanol and dried at air. Yield: 0.25g,(43%) and m.p = 150-152°C. Elemental analysis: (C.H.N Found, (Calc. %); C=68.35 (68.84), H= 5.92 (6.05), N=7.12(7.65),FT-IR data cm-1:3414 ν(O-H), 1685ν(C=O),1666,1620 δ(C=N), 1543ν(C=C)aromatic, 1238 ν (C-O), 1095 ν (C-N),3066 (C-H)aromatic, 2981(C-H)aliphatic.

Synthesis of Schiff-base ligand H2L

H2L was prepared according to the literature [12].3,3'-((1E,1'E)-(propane-1,diylbis(azanylylidene))bis(methanylylidene))bis (2-hydroxy-5-methylbenzalde hyde)) (0.5g, 1.4mmol)) in ethanol 15ml was added to an ethanolic solution 15ml of 4-Aminoantipyrine (0.56g, 2.8mmol) and the resultant mixture was refluxed for 5hr at 85°C with few drops HBr. The mixture was filtered off and washed in hot ethanol 15ml. The yellow solid formed as product, separated by filtration. Yield: 0.46g (46%), m.p 185- 187°C. Elemental analysis: (C.H.N Found, (Calc. %); C=69.89(70.09), H= 5.88 (6.02), N=15.00 (15.21), FT-IR data cm-1 :3417 ν(O-H), 1674ν(C=O), 1654 δ(C=N), 1589ν(C=C)aromatic, 1384 ν (C-O), 1238 ν (C-N),2924 (C-H) aliphatic, 2789(C-H)iminic.

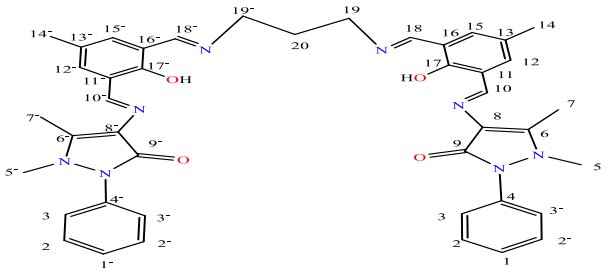

Fig.1: Chemical structure of ligand H_2L.

General synthesis procedure of the metal complexes

prepared according to the literature [13]. A mixture of the H_2L (1mmol) in ethanol 15ml containing KOH (2mmol) was added over 15min to a stirred solution of metal chloride (2mmol) in hot ethanol. The resulting mixture was refluxed for 4hr at 70-85°C, resulting in the formation of a coloured solution. The solution was concentrated by slow evaporation of the ethanol at RT. The solid mass formed was collected by filtration and washed with EtOH 10ml and finally with diethyl ether 15ml, (Scheme 1). Yields, Colours, Metal salts quantities, melting points for the complexes are listed in (Table 1).

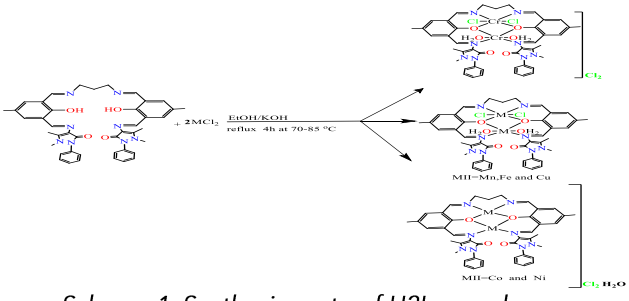

Scheme 1: Synthesis route of H2L complexes.

Table 1: Yields, Colours, Metal salts quantities, Melting points of complexes.

Complex	Weight of metal salt(g)	Weight of complex(g)	Yield (%)	color	m.p. °C
[Cr2(L)Cl2(H2O)2]. Cl2	0.18	0.2	58	Pale green	197
[Mn2(L)Cl2(H2O)2]	0.13	0.15	47	Brown	300*
[Fe2(L)Cl2(H2O)2]	0.14	0.17	53	Brown	250*
[Co2(L)] Cl2.H2O	0. 16	0.18	56	Light pink	300*
[Ni2(L)] Cl2.H2O	0.16	0.2	63	Dark green	250*
[Cu2(L)Cl2(H2O)2]	0. 11	0.18	55	Pale green	300*

Microbiological Evaluation

The sensitivity of bacteria and fungi against the prepared compounds were explored by Kirby-Bauer method. In this work, the colony of organism was mixed with a solution of 85% NaCl, until the interruption becomes (0.5 Mcf). This suspension was applied on the surface of a Petri dish filled with Mueller Hinton agar. The holes were made with the same space and exact concentration. Recommended concentration (100µL) of the test sample 1mg/mL in dimethylsulfoxide was introduced in the wells. The dishes were incubated for 24h at 37℃ and the inhibition zones were measured and compared with standard values [14]. The role of dimethylsulfoxide solutions in the microbiological evaluation were examined separately that indicated no activity against any bacterial strains or fungi species.

4. Results and Discussion

The new Schiff-base ligand is isolated in good yields from the reaction of the 4-aminoantipyrene with (3,3'-((1E,1'E) -(propane-1,3-diylbis (azanylylidene)) bis (methanylylidene))bis(2-hydroxy-5-methylbenzaldehyde).The ligand is prepared in two steps using ethanol as the reaction medium. The H_2L is a monobasic ligand that has the ability to form nuclear phenoxo-bridged complexes. The ligand is characterised by CHN, FTIR, UV-Vis and ^{1}H- NMR spectra. The metal complexes of Cr(Ш), Mn(II), Fe(II), Co(II), Ni(II) and Cu(II) were synthesised by reacting 1mmole of H_2L with 2mmole of the metal chloride, respectively, using ethanol as a medium, resulted in the isolation of six -coordinate monomeric compounds of the general formulae $[M_2(L)(H_2O)_2Cl_2].Cl_2$, M=Cr(Ш),$[M_2(L)Cl_2(H_2O)_2]$, M=Mn(II),Fe(II), $[M_2(L)]$ $Cl_2.H_2O$, M=Co(II),Ni(II), $[M_2(L)Cl_2].H_2O$, M= Cu(II). Scheme1. The solid complexes are stable and soluble only in DMF and in DMSO with heating, and not soluble in other common organic solvents. The solubility behavior may account for the formation of Schiff base species [15]. Eventually, upon complexation, the steric factors that facing the metal centers in the Schiff-base and the involvement of the 4-aminoantipyrene moiety in the coordination will avert the coordination of two binding atoms to a two-metal ion to form binuclear complexes. The expected geometries of the complexes were concluded from their spectral and other analytical information. The analytical data (Table 2). The assignments of the main FT-IR peaks of the ligand and their metal complexes are collected in (Table 3). The UV-Vis spectra of the ligand and their metal complexes are listed in (Table 4).

Table 2: Micro analysis and physical properties of complexes.

Complex	Molecular formula	M.Wt	Colour	m.p. °C	Yield (%)	Micro analysis found, (calculated)%				
						C	H	N	M	Cl
[Cr2(L)Cl2(H2O)2]. Cl2	C43H46Cl4Cr2N8O6	1016.68	Pale green	197	58	50.23 (50.80)	4.23 (4.56)	10.97 (11.02)	10.07 (10.23)	13.52 (13.95)
[Mn2(L)Cl2(H2O)2]	C43H46Cl2Mn2N8O6	951.67	Brown	300*	47	54.00 (54.27)	4.16 (4.87)	11.32 (11.77)	11.12 (11.55)	7.03 (7.45)
[Fe2(L) Cl2(H2O)2]	C43H46Cl2Fe2N8O6	953.48	Brown	250*	53	54.0 (54.17)	4.34 (4.86)	11.14 (11.75)	11.24 (11.71)	7.00(7.44)
[Co2(L)] Cl2.H2O	C43H44Cl2Co2N8O5	941.64	Light pink	300*	56	54.11 (54.85)	4.33 (4.71)	11.54 (11.90)	12.02 (12.52)	7.12 (7.53)
[Ni2(L)] Cl2.H2O	C43H44Cl2Ni2N8O	941.16	Dark green	250*	63	54.33 (54.88)	4.20 (4.71)	11.27 (11.91)	12.00 (12.47	7.01 7.53)(
[Cu2(L)Cl2(H2O)2	C43H46Cl2Cu2N8O6	968.88	Pale green	300*	55	53.00 (53.31)	4.12 (4.79)	11.11 (11.57)	12.95 (13.12)	7.01 (7.32)

FT-IR and NMR Spectra

he FT-IR spectra of the ligand exhibited prominent peaks at 3417,1674,1654,1589,1384 and 1238 due to ν(O-H), ν(C=O), ν(C=N), ν(C=C), ν(C-O) and ν(C-N), respectively [16-19]. After complexation, the FT-IR spectra of the metal complexes indicated bands with the appropriate shiftsthe M-N and M-O peaks that related to complexation (Table 3). Upon complexation, a band at 1674cm-1 attributed to ν(C=O) of the ligand carbonyl group, the carbonyl band is not the coordination of these moieties to the centre. The ν(C=N) of the imine groups is shifted and observed around 1620-1627 cm-1 in complexes indicating the coordination of the imine group to the metal atoms. These bands were moved to a lower frequency in comparison with that in the ligand. This is due to delocalisation of electron density (t2g) of the metal center to the π-system of the ligand [20-23]. The band at 1384cm-1 that due to ν(C-O) phenoxo in the ligand is shifted to a lower frequency, upon complexation and appeared about 1319-1384 cm-1 in the phenoxo-bridged complexes. This shift confirms the involvement of the phenoxo-oxygen atom in the coordination to the metal ion in a bridging mode [23]. The band at 1238cm-1 that due to ν(C-N) in the ligand is shifted to a higher frequency, upon complexation and appeared around 1238-1288cm-1 in the ν(C-N) complexes. This is in accordance with previous work reported in the literature [24]. The metal complexes spectrum revealed additional bands between (600-200) cm-1 that were not presented in the H2L spectrum. Bands related to ν(M-O) were detected range at (601-682) cm-1 [25]. The FT-IR spectra detected peaks correlated to ν(Cr-N), ν(Mn-N), ν(Fe-N), ν(Co-N),

v(Ni-N) and v(Cu-N),respectively, range at (478-405)cm-1[21-24].The FT-IR spectra revealed bands that belongs to v(Cr-Cl),v(Fe-Cl),v(Co-Cl) and v(Cu-Cl) at 287;239, 237;204, 262;227 and 275;227cm-1,respectively [25]. In complexes Mn (II), Fe (II), Ni(II) and Cu(II) a band that was detected at 775,810,732 and 744cm-1 is related to v(M-OH2). Finally, a band detected at 3448-3305cm−1 was correlated to aqua water molecules. The 1H NMR spectra of H2L is illustrated in (Fig 2). A signal at 9.46ppm that belongs to OH equivalent to two proton (2H, OH, s). A signal at 8.96ppm that belongs N=C-H (C10,10,)-H to proton of (2H, s) and a signal at 8.94ppm that belongs N=C-H (C18,18,)-H to proton of (2H, s). The chemical shift at 8.43-8.41ppm that equivalent to two proton and appear as single is related to (C15,15,)-H (2H, s). The chemical shift at 8.34-8.33ppm that equivalent to two protons and appears as a singlet is related to(C12,12,)-H (2H, s). The triplet peak at 7.74-7.72ppm that is equal to two protons are allocated to the (C2,2, 2,2,)-H ((4H, t, J=8Hz).The doublet peak at 6.17-6.15ppm that equivalent to protons assigned to the (C3,3, 3,3,)-H (4H,d,J =8Hz). The triplet peak at 6.14-6.11ppm that is equal to protons are allocated to the (C1,1,)-H (2H, t, J=12Hz).The triplet peak at 5.70-5.69ppm that equivalent to protons assigned to the -N-CH (C19,19,)-H (4H, t,J =4Hz). The single peak at 5.68-5.62ppm that equivalent to protons assigned to the -N-CH3(C5,5,)-H (6H, s).The single peak at 4.93-4.90ppm that equivalent to protons assigned to the -CH3(C7,7,)-H(6H,s).The single peak at 4.68-4.56ppm that equivalent to protons assigned to the -CH3(C14,14,)-H (6H,s).The miltplet peak at 1.12-1.10ppm that equivalent to protons assigned to the -CH(C20)-H (2H,m,J= 8Hz).

Table 3: The FT-IR spectral data of complexes (cm^{-1}).

Complex	ν(C=O)	ν(C=N) ν(C=C) aro	ν(C-O)	ν(C-N)	N (H2O) ν(M-OH2)	ν(M-O)	ν(M-N)	ν(M-Cl)
[Cr2(L)Cl2(H2O)2]. Cl2	1670	1624 1450	1319	1276	3394 775	632	474	287, 239
[Mn2(L)Cl2(H2O)2]	1670	1624 1546	1350	1238	3379 810	655	478	237, 204
[Fe2(L)Cl2(H2O)2]	1670	1620 1543	1384	1238	3414 732	601	459	262, 227
[Co2(L)] Cl2.H2O	1670	1620 1546	1350	1280	3448	663	416	-
[Ni2(L)] Cl2.H2O	1670	1624 1543	1384	1238	3444	682	459	-
[Cu2(L)Cl2(H2O)2]	1670	1627 1539	1381	1288	3305 744	632	405	275, 227

Mass spectrum

The mass spectrum of H2L a molecular weight peak at m/z = 736.86amu is not shown. The peak recorded in 683.51amu belongs to (C40H41N7O4), Fig (3) related to [M-(C40H41N7O4)]. The suggested fragmentation pattern is shown in Scheme (2). Peaks seen at 683.51(2.5%), 647.74(3%), 420.53(1%), 285.34(2%),105.11(4.2%) and 76.28(12.5) related to[M-(C40H41N7O4)],[M-(C40H41N7O4) + (C40H37N7O2+2)],[M-(C40H41N7O4) + (C40H37N7O2+2) +(C24H30N5O2+)], [M-(C40H41N7O4) + (C40H37N7O2+2) + (C24H30N5O2+) +(C15H20N3O+)],[M-(C40H41N7O4) + (C40H37N7O2+2)+(C24H30N5O2)+(C15H20N3O+) + (C7H5-)] and [M-(C40H41N7O4) + (C40H37N7O2+2) + (C24H30N5O2) + (C15H20N3O+)+(C7H5-)+(C6H6+2)], respectively, or [M-(C40H41N7O4)], [M-(C40H41N7O4) + (C40H37N7O2+2)],[M-(C40H41N7O4+2)+(C40H37N7O2+2) + (C11H16N+)], [M-(C40H41N7O4) + (C40H37N7O2+2)+(C11H16N+)+(C15H20N3O+)] and [M-(C40H41N7O4) + (C40H37N7O2+2)+(C24H30N5O2)+(C15H20N3O+) +(C6H6+2),respectively, and [M-(C40H41N7O4)],[M-(C40H41N7O4)+(C40H37N7O2+2)],[M-(C40H41N7O4)+(C40H37N7O2+2)+(C6H6+2)] respectively.

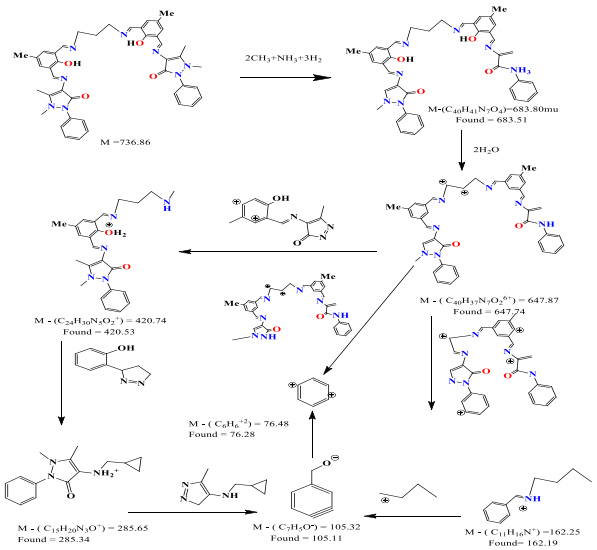

Scheme 2: The fragmentation pattern and relative abundance of H2L fragments.

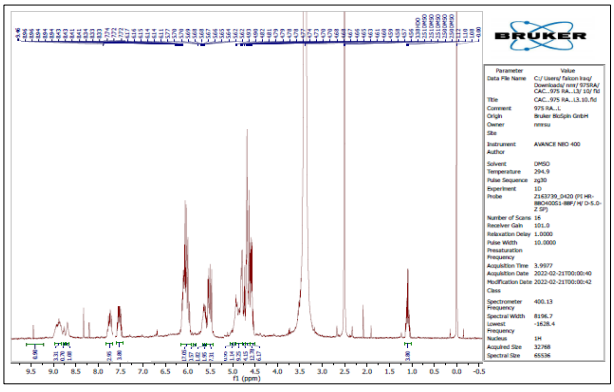

Fig 2: The ^{1}H-NMR spectrum of H_2L.

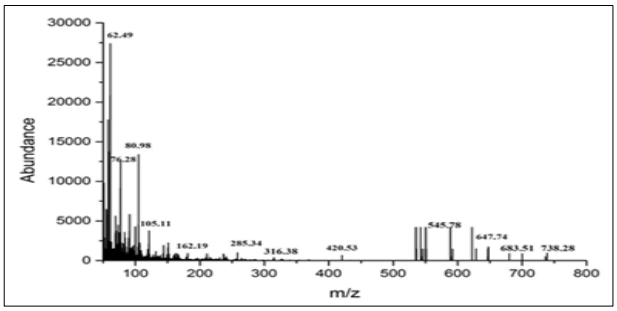

Fig 3: The electrospray (+) mass spectrum of H_2L.

Electronic spectra and magnetic moments measurements

The complexes' electronic spectra, magnetic moments measurements data are collected in (Table 4). Various peaks around 265-285nm are seen in the electronic spectra of the complexes, which are attributable to $\pi \rightarrow \pi*$ and $n \rightarrow \pi*$, respectively. Charge transfer (C.T) is responsible for additional peaks at 345-479nm [26, 27]. At 677nm, the electronic spectrum of Cr (III) exhibits band due to 4A2g→4T1g, revealing a deformed octahedral structure around the Cr (III) center. The deformed octahedral shape agrees with the magnetic moment value μeff =3.77BM of Cr (III). The electronic spectra of Mn (II) show a band in the d-d region at 720nm could be correlated to 6A1g→4T1g(4G), revealing a deformed octahedral structure. The measured magnetic moment value μeff =5.86BM is consistent with the Mn (II)-complex, which has a deformed octahedral configuration around the Mn atom. Fe (II) has band in the d-d region at 902nm that is visible in its electronic spectrum due to 5T2g →5Eg around the Fe (II)center, revealing a deformed octahedral structure. The measured magnetic moment value μeff=5.77BM is consistent with the Fe (II)-complex, which has a deformed octahedral configuration around the Fe atom [27,28]. At 536 and 680nm, bands in the Co (II)-complex assigned to 4A2(F)→4T1(P) and 4A2(F)→4T1(P), respectively were detected, indicating a tetrahedral geometry configuration around the metal center. The tetrahedral shape agrees with the magnetic moment value μeff =4.46BM of Co (II). Ni (II) complex spectrum revealed a peak at 423nm, which was attributed to 1A1g→1B1g. Ni-complex with square planer structure exhibit these transitions [27,29]. The square planer structure agrees with the magnetic moment value μeff diamagnetic of Ni (II). The electronic spectra of Cu (II) show a band in the d-d region at 891nm that is caused by 2Eg→2T2g, revealing a deformed octahedral structure The measured magnetic moment value μeff=1.81BM is consistent with the Cu (II)-complex, which has a deformed octahedral configuration around the Cu atom [27-29].

Table 4: The electronic spectra data of complexes, magnetic moment and conductivity.

Comp.	Band Position λnm	Wave number (cm 1)	Extinction coefficient εmax (dm3 mol-1 cm-1)	Assignment	μeff (BM)	Λm S.cm2.mole 1	Suggested geometry
$[Cr_2(L)Cl_2(H_2O)_2].Cl_2$	274 479 677	36496 20876 14771	2154 528 733	Intra-ligand π →π*, n→π* C.T $^4A_2g \rightarrow {}^4T_1g$	3.77	85	Distorted octahedral
$[Mn_2(L)Cl_2(H_2O)_2]$	267 363 720	37453 27548 13888	1375 113 33	Intra-ligand π →π*, n→π* C.T $^6A_1g \rightarrow {}^4T_1g^{(4G)}$	5.86	21	Distorted octahedral
$[Fe_2(L)Cl_2(H_2O)_2]$	271 345 902	36900 28985 11086	1968 2034 11	Intra-ligand π →π*, n→π* C.T $^5T_2g \rightarrow {}^5Eg$	5.77	7	Distorted octahedral
$[Co_2(L)].Cl_2.H_2O$	267 463 536 680	37453 21598 18656 14705	691 13 31 100	Intra-ligand π →π*, n→π* C.T $^4A_2{}^{(F)} \rightarrow {}^4T_1{}^{(p)}$ $^4A_2{}^{(F)} \rightarrow {}^4T_1{}^{(p)}$	4.46	77	Tetrahedral
$[Ni_2(L)]$ Cl2.H2O	265 354 423	37735 28248 23640	875 111 123	Intra-ligand π →π*, n→π* C.T $^1A_{1g} \rightarrow {}^1B_{1g}$	Diamagnetic	74	Square planer
$[Cu_2(L)Cl_2(H_2O)_2]$	285 348 891	35087 35087 11223	2434 2496 73	Intra-ligand π →π*, n→π* C.T $^2Eg \rightarrow {}^2T_2g$	1.81	19	Distorted octahedral

Thermal Analysis

The thermal decomposition analysis of solid ligand H2L was carried out under argon atmosphere. The TGA data clearly indicated that the decomposition of the ligand proceeds in two steps, Fig (4). The weight loss at the 1st peak, as indicated by the TGA curve at 40-248°C,many attribute to the loss of (CO+4H2+NH3+2CH4+2C2H6)segments (obs.=0.1647mg,19.71%;calc.=0.1643mg,19.67%).The second step recorded at 248-896°C may indicate the loss of (2CN+C4H7N4) segments,(obs.=1.8577mg,22.23%;calc=1.8485 mg,22.12%). The residual weight loss, as indicated by the TGA curve many attributes to the loss of (C30H6+NO3) segments, (calc.=5.5692mg,58.20%). The 1st peak may relate to the melting point of the ligand. The thermogram [Co2(L)Cl2].H2O complex is proceeds in three steps, (Fig 5). The first step detected at 42-249 °C may be attributed to the loss of a molecule of the (H2O+2CO+H2) segments; (obs.=0.7676mg,8.1%; calc.=0.7647mg, 8.07%). The

second step recorded at 249-616°C indicated the loss of (3CN+CH4) fragments,(obs.=0.9477mg,10%;calc.= 0.9477mg, 10%).The third step recorded at 616-899°C indicated the loss of (C2H5) fragment,(obs.=0.3013mg,3.18%;calc.=0.2918mg,3 .08%).The residual weight loss, as indicated by the TGA curve many attribute to the loss of (3C6H6+5CN+C13H13+Co2O2+Cl2) segments,(calc.=7.473mg, 78.86%).The 1st peak may relate to the melting point of the complex. The thermogram [Ni2(L)] Cl2.H2O complex is proceeds in three steps, (Fig 6). The first peak detected at 41-297°C may be attributed to the loss of a molecule of the (H2O+2CO+2NH3+CH4) segments; (obs. =4.626mg, 13.22%; calc.=4.608mg, 13.17%). The second step recorded at 297-484°C indicated the loss of (4CN) fragment, (obs.=3.894mg 11.13%; calc.= 3.866mg,11.05%). The third step recorded at 484-898°C indicated the loss of (Cl+H2) fragments, (obs.=1.378 mg, 3.94%; calc.=1.375mg, 3.93%).The residual weight loss, as indicated by the TGA curve many attribute to the loss of (Ni2O2+6C6H5+N2+Cl) segments,(calc.=25.19mg,71.84%) and The thermogram [Cu2(L)Cl2(H2O)2] complex is proceeds in three steps, (Fig7). The first step detected at 41-203°C may be attributed to the loss of a molecule of the (2CO+2H2O +CH4+H2) segments; (obs. =1.088mg,11.36%;calc.=1.087mg, 11.35%).The second step recorded at 203-497°C indicated the loss of(2CN+2NH3+C2H6)fragments,(obs.=1.156mg12. 07%;calc.=1.149mg, 12%).The third step recorded at 497-899°C indicated the loss of (4CN+Cl2+5H2) fragments, (obs.=1.820mg,19.00%; calc.=1.819mg,18.99%).The residual weight loss, as indicated by the TGA curve many attribute to the loss of (Cu2O2+2C6H4+C20H6)segments,(cala..=5.525mg , 42.31%).

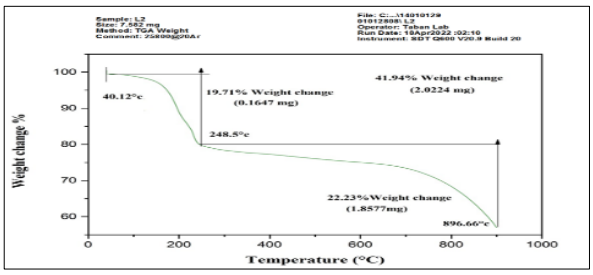

Fig 4: The thermal curves TGA of H_2L in Ar atmosphere.

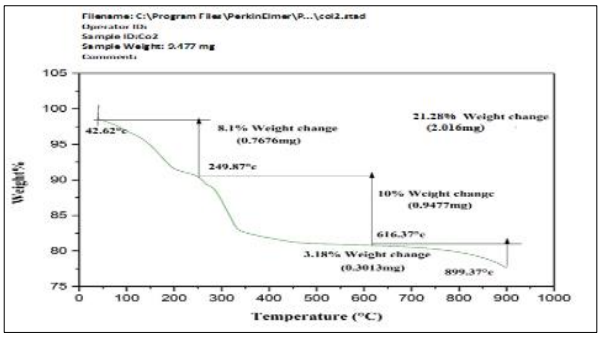

Fig 5: The thermal curves TGA of [$Co_2(L)Cl_2$]. H_2O in Ar atmosphere.

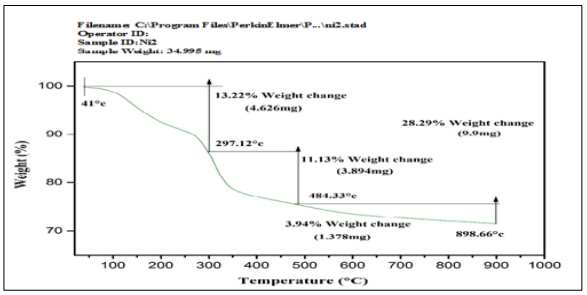

Fig 6: Thermal decomposition of [$Ni_2(L)$] Cl_2. H_2O in Ar atmosphere.

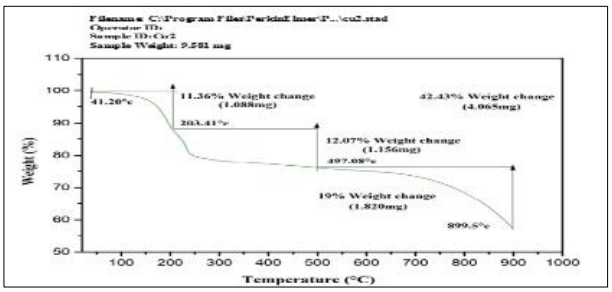

Fig 7: Thermal decomposition of [$Cu_2(L)Cl_2(H_2O)_2$]in Ar atmosphere.

5. Biological Activity

The antibacterial evaluation of the synthesised ligand H2L and its metal complexes with Cr(Ш), Mn(II), Fe(II), Co(II), Ni(II) and Cu(II)) ions were tested against four types of bacteria: Staphylococcus aureus, Bacillus subtilis, Escherichia coli, and Pseudomonas aeruginosa subtilis Separate investigations carried out using DMSO solutions alone revealed no action against any bacterial strains, confirming the significance of DMSO in biological screening [30-32]. Table (5) shows the results of the tests against the development of several bacterial strains. The impact of the produced ligand and its complexes on the microorganisms under investigation is depicted.The recorded results indicated that complexes were found to be more active; the experimental results concluded the following:

1.All complexes showed activity against positive and negative bacteria.

2.Based on the information gathered, Cr (III) and Cu (II) complexes shows the higher microbiological activity against strains of ((Staphylococcus aureus, Bacillus subtilis) and (Escherichia coli, Pseudomonas auroginosa) bacterial, whereas Mn (II), Fe (II),Co(II) and Ni(II) complexes is less effective against ((Staphylococcus aureus, Bacillus subtilis) and (Escherichia coli, Pseudomonas auroginosa) bacterial.

3.The metal complexes of H2L showed a good exhibit antibacterial activity that is well-matched with Cefotaxime, which would lead to the potential biomedical applications of the prepared complexes. The antifungi evaluation of the synthesised ligand H2L and its metal complexes with Cr(Ш), Mn (II), Fe (II), Co (II), Ni (II) and Cu (II)) ions was tested against two types of fungi (Candida albicans and Rhizopus sporium). Separate investigations carried out using DMSO solutions alone revealed no action against

fungi organism, confirming the significance of DMSO in biological screening [31-33]. Table (6) shows the results of the tests against the development of two fungi organism. The impact of the produced ligand and its complexes on the microorganisms under investigation is depicted.The recorded results indicated that complexes were found to be more active; the experimental results concluded the following:

1.All complexes showed activity against fungi organism.

2.Based on the information gathered, Mn (II) and Cu (II)complexes showed the higher microbiological activity against two types of fungi (Candida albicans and Rhizopus sporium), whereas Cr (III), Fe (II), Co(II) and Ni(II) complexes are less effective against (Candida albicans and Rhizopus sporium), the tested fungi.

3.The metal complexes of H2L showed a good exhibit, that is well-matched with the Fluconazole,which would lead to the potential biomedical applications of the prepared complexes.

Table5: The inhibition zones (mm) of anti-bacterial activity for ligand and thier complexes.

Compounds	Escherichia coli (G−)	Pseudomonas aeruginosa(G−)	Staphylococcus aureus (G+)	Bacillus stubtilis (G+)
DMSO	-	-	-	-
(Cefotaxime)	17	21	18	15
H2L	16	15	22	17
[Cr2(L)Cl2(H2O)2]. Cl2	19	18	38	22
[Mn2(L)Cl2(H2O)2]	16	17	19	17
[Fe2(L) Cl2(H2O)2]	16	12	24	17
[Co2(L)] Cl2.H2O	15	17	17	20
[Ni2(L)] Cl2.H2O	16	18	18	13
[Cu2(L)Cl2(H2O)2]	19	23	21	21

Table6: The inhibition zones (mm) of anti-fungal activity for ligand and thier complexes.

Compounds	Candida albicans	Rhizopus sporium
DMSO	--	--
Fluconazole	10	10
[Cr2(L) Cl2(H2O)2]. Cl2	25	15
[Mn2(L) Cl2(H2O)2]	28	25
[Fe2(L) Cl2(H2O)2]	25	20
[Co2(L)] Cl2.H2O	20	15
[Ni2(L)] Cl2.H2O	20	15
[Cu2(L)Cl2(H2O)2]	33	32

6. Conclusion

The synthesis of new Schiff-base ligand that are capable to form metal complexes and their coordination chemistry with Cr(Ш), Mn (II), Fe (II), Co(II), Ni(II) and Cu(II)) ions are investigated. Schiff-base ligand with the title metal ions resulted in the fabrication of metal complexes. The coordination sphere and type of bonding of the complexes were examined using a range of analytical and spectroscopic techniques. These approaches indicated the fabrication of metal complexes, in which the geometries around metal centers are four and six-coordinate complexes were created. Biological evaluation of ligand and their metal complexes against gram-positive bacteria (G+), (Bacillus stubtili, Staphylococcus aureus and gram-negative bacteria (G−), Escherichia coli and Pseudomonas aeruginosa) and compared with antibiotic drug (Cefotaxime) and two types of fungi namely (Candida albicans and Rhizopus sporium) and compared with the activity of fungal agent (Fluconazole). The collected data revealed the antimicrobial activity of the ligand was enhanced upon complex formation.

References

1. M. Chatterjee and Saktiprosad Ghosh, 1998. Trans. Met. Chem, 23,355.

2. J. March 1979. Advanced Organic Chemistry Third edition, John Wiley and Sons. Inc, New York.

3. Mohammed, L.A, Mahdi, N.I. and Aldujaili, R.A.B, 2020. Preparation, characterization and the biological activity study of a new heterocyclic (Azo-Schiff base) ligand and their complexation with {Co, Ni, Cu, Zn (II)} ions. Egyptian Journal of Chemistry, 63(1), pp.289-300. 4. El-Kholy, N.G, 2017. Synthesis, Spectroscopic characterization, Antimicrobial, Antitumor Properties of new 4-amino-2, 3 dimethyl-1-phenyl-3-pyrazolone-5-one (antipyrine) Schiff bases and its transition metal complexes. Journal of American Science, 13(2), pp.132-145.

5. AbdulReda, N.A. and Abdulameer, S.R, 2018. Synthesis and characterization of some New derivatives of 8-chlorotheophyline by Micro-wave-Assist Suzuki-Miyaura coupling react-ion. Pak. J. Biotechnol, 15.

6.Khdur, R.A. and Zimam, E.H, 2018. Synthesis and characterization of some new β-lactam derivatives from azo sulphadiazine and its biological evaluation

as anticancer. Oriental Journal of Chemistry, 34(1), p.371.
7. Kurdekar, G.S, Sathisha, M.P, Budagumpi, S, Kulkarni, N.V, Revankar, V.K. and Suresh, D.K,2012. 4-Aminoantipyrine-based Schiff-base transition metal complexes as potent anticonvulsant agents. Medicinal Chemistry Research, 21(9), pp.2273-2279.
8. Hossain, M.S, Roy, P.K, Zakaria, C.M. and Kudrat-E-Zahan, M, 2018. Selected Schiff base coordination complexes and their microbial application: A review. Int. J. Chem. Stud, 6(1), pp.19-31.
9. Kumar, H. and Chaudhary, R.P, 2010. Biological studies of a novel azo based Heterocyclic Schiff base and its transition metal complexes. Der Chemica Sinica, 1(2), pp.55-61.
10. Khdur, R.A. and Zimam, E.H, 2018. Synthesis, characterization and study biological screening of some new azetidinone derivatives from azo sulphadiazine. Pak. J. Biotechnol, 15(1), pp.201-217.
11. Gedye, R, Smith, F, Westaway, K, Ali, H, Baldisera, L, Laberge, L. and Rousell, J, 1986. The use of microwave ovens for rapid organic synthesis. Tetrahedron letters, 27(3), pp.279-282.
12. Giguere, R.J, Bray, T.L, Duncan, S.M. and Majetich, G, 1986. Application of commercial microwave ovens to organic synthesis. Tetrahedron letters, 27(41), pp.4945-4948.
13.. MJ Al-Jeboori, AH Al-Dujaili, AE Al-Janabi (2009) Coordination of carbonyl oxygen in the complexes of polymeric Ncrotonyl-2-hydroxyphenylazomethine, Transition Met. Chem, 34: 109-113.
14. Kuhnert, N, 2002. Microwave-assisted reactions in organic synthesis-are there any nonthermal microwave effects? Angewandte Chemie International Edition, 41(11), pp.1863-1866.
15. Koldobskii, G.I, Ostrovskii, V.A. and Gidaspov, B.V, 1980. Tautomerism and acid-base properties of tetrazoles. Chemistry of Heterocyclic Compounds, 16(7), pp.665-674.
16. Ramesh, R. and Maheswaran, S, 2003. Synthesis, spectra, dioxygen affinity and antifungal activity of Ru (III) Schiff base complexes. Journal of inorganic biochemistry, 96(4), pp.457-462.
17. Koldobskii, G.I, Ostrovskii, V.A. and Gidaspov, B.V, 1980. Tautomerism and acid-base properties of tetrazoles. Chemistry of Heterocyclic Compounds, 16(7), pp.665-674.
18. Nair, M.S, Arish, D. and Johnson, J, 2016. Synthesis, characterization and biological studies on some metal complexes with Schiff base ligand containing pyrazolone moiety. Journal of Saudi Chemical Society, 20, pp. S591-S598.
19. SilverschtienR.M, Bassler and Morril, 1981. Spectrophotometers Indentification of Organic Compound, Translated by Ali Hussain and Suphi Al-Azawi.
20. Enaam I. Y.2018.Journal of Global Pharma Technology. 10(03):875-882.
21.Hasan A. H, Enaam I.Y and Ahmed K. H. 2020. Journal of Plant Archives, 20 (1). pp. 2405-2411.
22. Faliah Hassan Ali Al-Jeboori, Mohamad Jaber Al-Jeboori and Abdul Muhsin Al-Haidari, 2013.Synthesis and structural characterization of some transition metal complexes with cyclic N2OS2 ligand, J. Chem. Pharm. Res, 5(8), 203-216..
23. F. H. A. Al-Jeboori, K. K. Hammud, M. J. Al-Jeboori, 2014. Synthesis and characterization of new acyclic octadentate ligand and its complexes,Iranian Journal for Science & Technology, 38A (4): 489-497.
24.A. L. Pochodylo, R. L. LaDuca, 2011. Inorg. Chem. Comm, 14, 722-726.
25. M. Tumer, C. Celik, H. Koksal, S. Serin. 1999.Transition Met. Chem, 24, 525.
26.Safaudeen A. Hussain and Mohamad J. Al-Jeboori, 2019.New Metal Complexes Derived from Mannich-Base Ligand; Synthesis, Spectral Characterisation and Biological Activity, Journal of Global Pharma Technology, 11(2), 548-560,
27.Sharghi, H, & Jokar, M,2010. Highly stereoselective facile synthesis of β-amino carbonyl compounds via a Mannich-type reaction catalyzed by γ-Al2O3/MeSO3H (alumina/methanesulfonic acid: AMA) as a recyclable, efficient, and versatile heterogeneous catalyst. Canadian Journal of Chemistry, 88(1), 14-26.
28. Ramachandran, E, Gandin, V, Bertani, R, Sgarbossa, P, Natarajan, K, Bhuvanesh, N. S, & Marzano, C.2018. Synthesis, characterization and cytotoxic activity of novel copper (II) complexes with aroylhydrazone derivatives of 2-Oxo-1, 2-dihydrobenzo[h] quinoline-3-carbaldehyde. Journal of Inorganic Biochemistry,182, 18-28.
29. Ho J, Lee WY, Koh KJT, Lee PPF, Yan YK. 2013.Rhenium(I) tricarbonyl complexes of salicylaldehyde semicarbazones: Synthesis, crystal structures and cytotoxicity, Journal of Inorganic Biochemistry, 119: 10-20.
30.Lever, 1984.A. P. Inorganic electronic spectroscopy. Studies in physical and theoretical chemistry, 33.
31.Al-Jeboori M. J, Hasan H. A. and Yousif E. I, 2012. Metal-assisted assembly of dinuclear metal(II) dithiocarbamate Schiff-base macrocyclic complexes: Synthesis and biological studies, Global J. Inorg. Chem, 3. 10. 1-7.
32.. Enaam Ismail Yousif, Nihad Kadhum Hasan and Mohamad J. Al-Jeboori.2022. New Metal Complexes of Thiosemicarbazone Mannich base Ligand; Synthesis, Structural Characterisation and Biological Activity P J M H S Vol. 16, No. 06, 565.
33.Yousif. E. I, New Mixed Ligand Complexes; Synthesis, Spectral Analysis and Biological Activity. Journal of Global Pharma Technology, 2019. 11(02) :P.196-203.